Reduction Evaluation and Management of Agricultural Non-Point Source Pollutant Loading in the Huntai River Watershed in Northeast China

Yicheng Fu, Wenqi Peng*, Xiaoyu Cui, Jinyong Zhao

State Key Laboratory of Simulation and Regulation of River Basin Water Cycle, China Institute of Water Resources and Hydropower Research

* Corresponding author, E-mail: pwq@iwhr.com

Abstract:

With the raise of environmental protection awareness, applying models to control non-point source (NPS) pollution has become a key approach for environmental protection and pollution prevention and control in China. In this study, we implanted the semi-conceptual model Soil and Water Assessment Tool (SWAT) using information on precipitation runoff, land use, soil and slope. The model was used to quantify the spatial loading of NPS nutrient total nitrogen (TN) and total phosphorus (TP) to the Huntai River Watershed (HTRW) under two scenarios: without and with projected buffer zones of approximately 1 km within both banks of the Huntai, Taizi and Daliao river trunk streams and 5 km around the reservoirs. Current land-use types within the buffer zone were varied to indicate the natural ecology and environment. The Nash-Sutcliffe efficiency coefficient (E_{NS}) and R^2 for flow and predicted nutrient concentrations (TN and TP) in a typical hydrological station were both greater than 0.6, and the relative deviation ($|Dv|$) was less than 20%. Under the status quo scenario (SQS), the simulated soil erosion in the HTRW per year was 811 kg/ha, and the output loadings of TN and TP were 19 and 7 kg/ha, respectively. The maximum loadings for TN and TP were 365 and 260 kg/ha,

respectively. Under environmental protection scenarios (EPS), the TN and TP pollutant loadings per unit area were reduced by 26% and 14% annually, respectively. Loading analysis showed that land-use type is a key factor controlling NPS pollution. The NPS pollutant loading decreased under the simulated EPS, indicating that environmental protection measures may reduce the NPS pollutant loading in HTRW. The 22% pollutant reduction under the EPS. We finally quantified the ratio of the land area lost to agricultural production compared with that lost to ecosystem services. We calculated the agricultural yield elasticity and concluded that the corresponding crop yield would be reduced by 2% when the land area for ecosystem services in the basin increased by 1% under the EPS.

Keywords:

Agricultural Non-Point Source pollutant loading; Environmental Protection Scenarios; Agro-ecosystem services; Huntai River Watershed

1. Introduction

The non-point source (NPS) pollution strongly influences soil restoration, people living environments and water quality safety. Many articles have indicated that underlying surface conditions and rainfall features will affect the spatial distribution characteristics of NPS pollution nutrient loading (Robinson et al.,2005). Pollutant loadings from different land-use types vary significantly (Niraula et al.,2013). The NPS pollutant concentration in water depends on the discharge loading and pollutant treatment rate. Presently, a lot of academics prefer loadings over concentrations to express their study (Yang et al., 2007; Ouyang et al.,2010; Outram et al., 2016). Land-use types and underlying surface status will impact the nutrient resources and spatial distribution characteristics (Ahearn et al., 2005; Ouyang et al., 2013). The spatial-temporal characteristics of NPS pollutants can be studied based on panel data statistical

47 analysis and multi-model simulation. The SWAT model can be implemented for NPS pollutant
48 loading and provide the optimization programme for comprehensive ecological protection of
49 watershed (Shen et al.,2011). A large number of literatures have demonstrated that combining
50 different land use scales, land coordinated development patterns and geomorphologic landscape
51 characteristics can decrease NPS pollution loadings (Sadeghi et al.,2009).

52 Distributed physically-based and semi-conceptual models can effectively calculate and
53 evaluate NPS pollution loading spatial layouts. In the late 20th century, American scientists at
54 United States Department of Agriculture-Agricultural Research Service (USDA-ARS)
55 developed the SWAT model (Arnold et al.,1998), which has been widely used to simulate
56 runoff, estimate NPS pollution loading and implement Best Management Practices (BMPs).
57 SWAT is comprehensively used in evaluating the influence of NPS pollution loading on
58 different regional natural landscape characteristics and land-use types, including vegetation
59 coverage, underlying surface, agricultural generation modules and hydrometeorology data. The
60 changes of agricultural NPS contaminations based on the diversification of land development
61 types have been analyzed and researched by SWAT models (Ficklin et al.,2009; Shen et al.,
62 2013). The SWAT model's main body contains 80 mathematical equations and 530 intermediate
63 variables, which have been widely used to determine and evaluate NPS pollutant loading spatial
64 distribution characteristics to quantitative the impacts of land use on NPS pollutants and soil-
65 water loss sensitive evaluation on a watershed scale (Gosain et al.,2005; Ouyang et al., 2009;
66 Logsdon et al.,2013).

67 HTRW is the basic product manufacturing base in China and a primary tributary of the Liaohe
68 River Basin, which has been heavily polluted in recent years. The main NPS pollution in the
69 Liaohe river is agricultural NPS pollution, and most NPS pollution occurs in the HTRW within

Liaoning province (Liaoning Province DEP, 2011). Therefore, the HTRW faces enormous pressure from water pollution risk. The policy of 'Revitalization of Old Industrial Bases in Northeast China' has caused great spatial pattern changes to the land-use (Liu et al.,2014). This accelerating urbanization changes the current land use in a way that results in more NPS pollution to local surface waters.

The SWAT model was applied to quantify the TN and TP output loading in HTRW under different land uses, assess the NPS pollutant loading reduction, and analyse the spatial distribution characteristics under the condition of land cover change. Using SWAT, nutrient losses were simulated and evaluated under two scenarios: the status quo scenario (SQS, without buffer zones) and the 'environmental protection' scenario (EPS, with buffer zones). We studied NPS pollution problems in HTRW according the following steps and illustrated in the Fig. 1: (1) define the underlying surface (land-use) status for HTRW; (2) implement a SWAT model to simulate the NPS pollution loading (TP and TN) of the HTRW under two scenarios; (3) compare the NPS pollution loading under the two scenarios and assessed the effect of reducing pollutant loading under EPS; and (4) analysed the correlation between arable land area decrease/agro-ecosystem services increase and crop yield reduction using a simple static model.

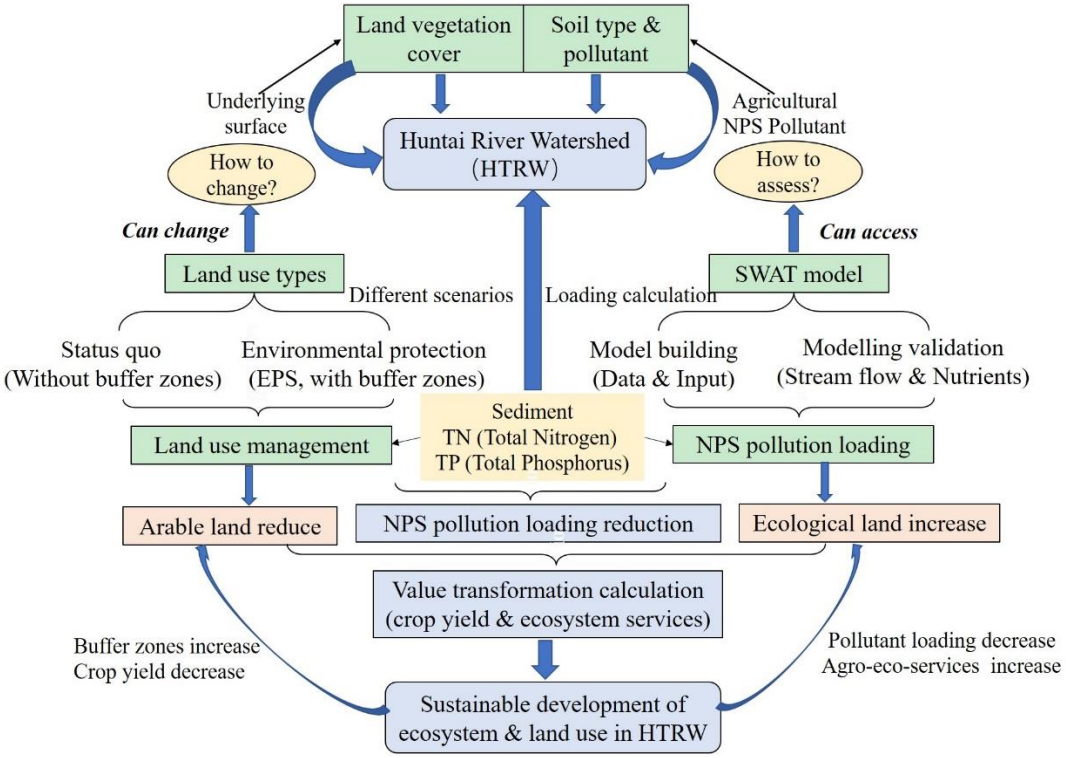

Fig. 1. Reduction assessment and value transformation system for agricultural NPS loading. The solid thick arrows indicate the degree of influence or the process output. The thin arrows indicate the process input.

2. Materials and methods

2.1 Huntai River Watershed

The HTRW (40°27'~42°19'N, 121°57'~125°20'E) is situated in the Liaoning province (Northeast China), and the river basin area is 2.73×10^4 km^2, which comprises approximately 1/5 of the Liaoning province (Fig. 2). The HTRW is a tributary of the Liaohe River (one of China's larger water systems) and consists of the Hunhe, Taizi, and Daliao Rivers. The Taizi River, Hunhe River, and Daliao River watersheds are the HTRW's sub-catchments. The HTRW varies topographically with low mountains in the eastern portion and alluvial plains in the other areas. The northeast region has a high elevation. Loamy soils are mainly distributed in the alluvial plain, and the average slope in the lower HTRW is

approximately 7%. The HTRW area consists of the cities of Shenyang, Fushun, Liaoyang, Anshan, Benxi, and Yingkou, most of Panjin city. Stream flow and nutrients were measured on five monitoring stations: Beikouqian, Dongling Bridge and Xingjiawopeng in the Hunhe River and Xialinzi and Tangmazhai in the Taizi River. HTRW has a temperate continental climate with an average annual temperature of 7°C and precipitation of 748 mm.

The HTRW is in a conventional agricultural farming (farming-dominated products), with much of the farmland dominated by crops. The total farmland area is 10,763 km^2 (39% of the total area), including 4,086 km^2 of paddy fields (dominated by rice) and 6,677 km^2 of dry farmland (including corn, soybean, vegetables and other crops). The upper Hunhe and Taizi river areas are mountains (69%), plainlands (25%) and low hills (6%). The HTRW's economic output value is dominated by agricultural cultivation. The farmland is mainly distributed in the alluvial plain area and valleys in riverine belts. Considering land use, pollutant sources and rainfall, the HTRW faces a high risk of agricultural pollution. Heavy fertilizer use and soil erosion in the upper HTRW has led to its heavy water pollution. For example, the Dahuofang reservoir (located in the middle reaches of Hunhe River) and the water resources-environment conservation area in its upper sections are facing serious threats, and the agricultural NPS pollution is becoming increasingly severe with no effective controls. Fertilization in the HTRW is predominantly nitrogen, followed by potassium and phosphorous. Heavy use of chemical fertilizers includes mainly DAP (diammonium phosphate), urea and a small amount of N-P-K (nitrogen-phosphorus-potassium mixed fertilizer). Acetochlor and Atrazine are mainly used on dryland, and Butachlor is mostly used in paddy soil. Based on 2006-2012 statistical information, the fertilizer and pesticide quantities (such as Methamidophos and Plifenate) used in the watershed fluctuated annually. The upper portions of the Huntai and Taizi Rivers are dominated

by mountains, and the crops are cultivated and harvested by hand. We obtained these data and information, which would normally be inaccessible, through onsite investigations, inquiry visits, case studies, example analyses. At present, farmland weeds and pests are mainly controlled by pesticides and herbicides. The upstream is rich in forest resources, and the downstream has a large amount of farmland. Special landscape layout makes the HTRW a potential area for agricultural NPS pollution. The reservoir outflow was used as an input into SWAT.

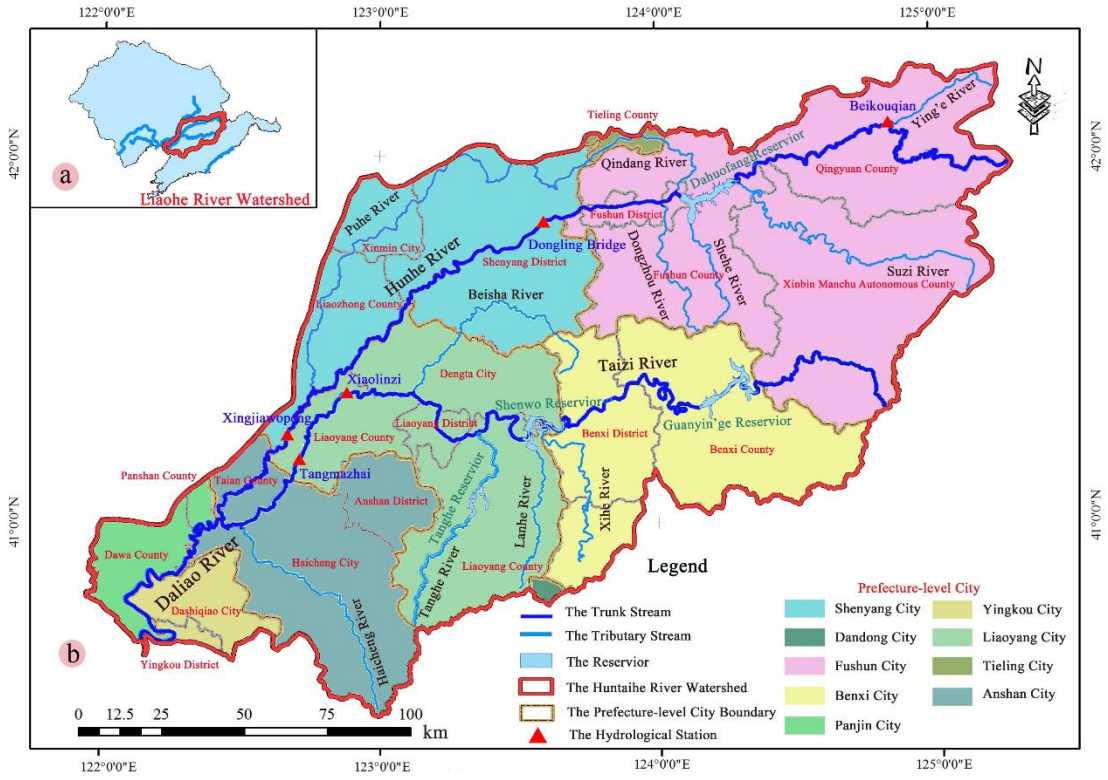

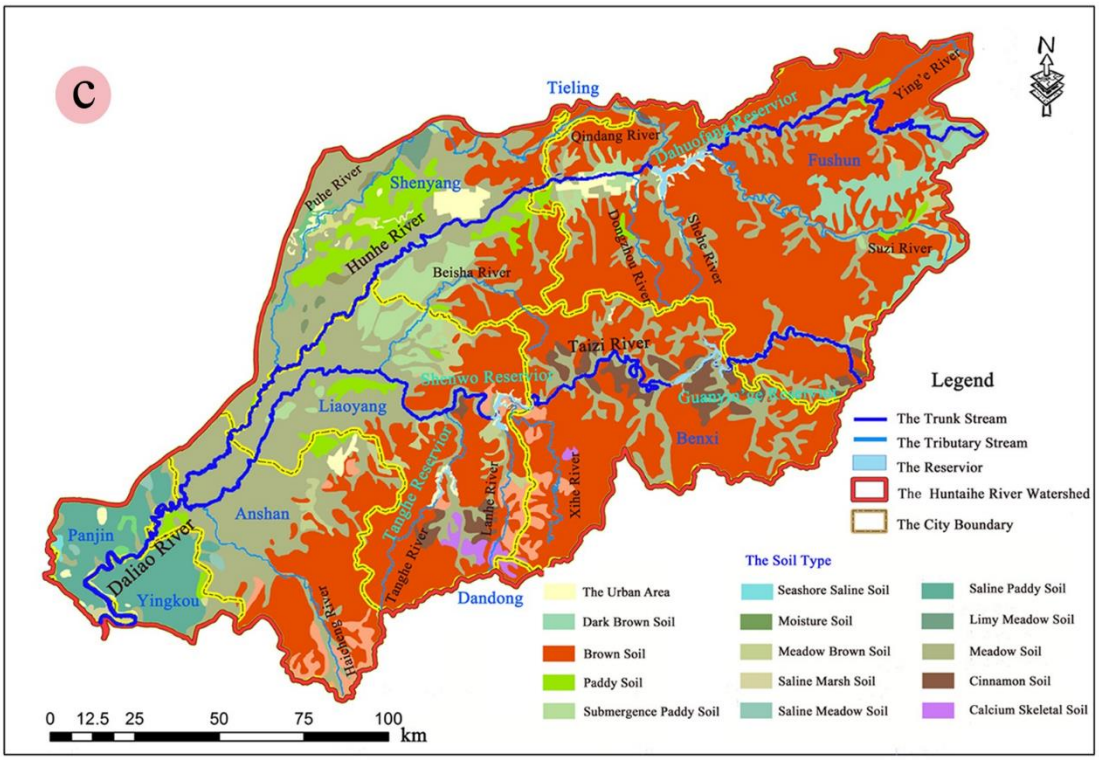

129

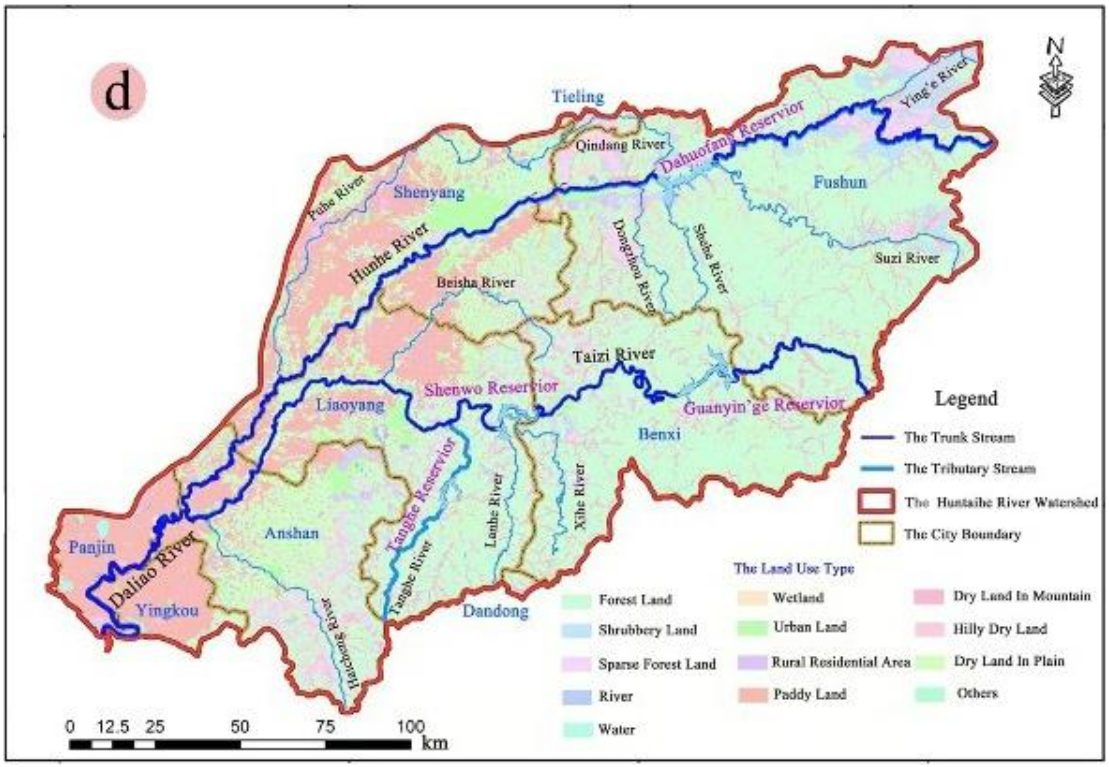

130

131 **Fig. 2.** Basic HTRW information. a. Location of the HTRW; b. Geographical zoning of HTRW;

132 c. Land use type of HTRW; d. Soil type of HTRW. The figure was cited from www.geodata.cn,

which is a national science and technology basic conditions platform and an earth system science data sharing platform. The figure information is public. The Liaoning province Water Resources Administrative Bureau granted permission for the basic information on the HTRW.

2.2 Setting the scene

To determine the correlation between land use types and agricultural NPS pollutant loading, the numerical analysis and comprehensive comparison method was used for different land use types under ecological development and urbanization. In this study, two scenarios were developed: The status quo scenario (SQS) and the environmental protection scenarios (EPS).

The SQS was draw up based on the current environmental protection mode and socioeconomic developmental structure. The land-use was based on the existing development pattern and environmental protection policies. BMPs information and environment-friendly land-use patterns (amount of pesticide and fertilizer used, cultivated land area, and crop species) were gained from Liaoning Province statistical yearbooks-2013 and field surveys of land consolidation.

The EPS was defined as considering the regional developmental prospects, eco-friendly environment restoration strategy of the HTRW. Buffer zones were defined as One kilometer within both banks of the Hunhe, Taizi and Daliao rivers (the width of the Buffers was One kilometer, the length was the same as the river) and 5 km around the reservoirs. In the buffer zones, traditional land-use patterns were changed to restore the natural landscape (forest and grassland) and ecological environment. This scenario is not only expected to preserve the fundamental agricultural position in the watershed but also to improve the watershed's ecosystem service value and biodiversity by reducing the amount of fertilizers and pesticides used for agricultural productivity. These scenarios can provide a scientific basis for further understanding characteristics of the nitrogen and phosphorus loading characteristics and

cultivated field plantation potential adjustment in HTRW.

To simulate the hydrological characteristics by SWAT, we first divided the HTRW into a set of sub-basins based on DEM data. We then divided sub-basins into Hydrological Response Units (HRUs). Hunhe River, Taizi River, and Daliao River sub-catchments were delineated into DEM and river system and further divided by 29 small calculation modules based on 184 HRUs. The downstream of Hunhe River, Taizi River, and Daliao River has little change in terrain, the direction of water flow is single, and the source of contaminant is relatively stable. Therefore, some small calculation units are combined during the calculation process to reduce calculation time and improve operating efficiency. We used the monitored data to calibrate and validate the stream flow and pollutant concentration changes in the HTRW. The land development patterns in the two scenarios were then input to the SWAT model to simulate the TN and TP pollutant loading. Finally, the spatial dynamics and ecological service value assessment in NPS pollution loading was analysed based on land-use. We also analyzed the negative correlation between the agro-ecological value and the farmland area.

The wastewater pollutant source is along both channels of the Taizi, Hunhe, and Daliao River trunk streams. The risk of NPS pollution is mainly related to the patterns of farmland use and agricultural planting. The secondary region for water pollution is mainly along the HTRW tributaries. Therefore, we paid special attention to the comparative analysis of pollutants generated by the cultivated field adjacent to the water channels.

2.3 Methods

2.3.1. SWAT principle

SWAT is a semi-physical and distributed hydrological model developed to quantitatively predict the responsivity of water quality and quantity to land-use and environmental protection

methods on a watershed scale (Gassman et al.,2007). The primary data imported to run the model includes soil type, vegetation status/land landscape, DEM (Digital Elevation Model)/topography, and BMPs. The watershed SWAT model's computing units are the sub-watershed scale and HRUs. Hydrological response unit demarcation is based on land use, soil type and slope.

SWAT HRUs are automatically divided by geomorphological features, land development intensity change, DEM, and soil conditions. To calculate the HRUs, we selected 0% land use, slope/elevation, and soil classification/attributes as the initial value on the HTRW scale. Therefore, 184 HRUs were delineated to determine NPS pollutant loading. HRUs are the minimum units for predicting pollutant output loading, which is automatically generated by superimposing land-use and soil types within the sub-river basin. Due to the HTRW's large area and widely changing terrain slope, the HTRW was divided into three levels with slopes of 10 and 30 nodes. The area threshold percentages for land use, soil and slope were 5%, 8%, and 15%, respectively. To evaluate pollutant loss and spatial characteristics, the soil nutrient loss curve, water-salt balance equation, and stage-discharge curve were applied. Meteorological data (the min and max temp is -30℃and 40℃, respectively) were gained from automatic weather stations and hydrological station network in 12 cities within the HTRW. BMP data, such as crop irrigation time (late April and early May) and water, crop harvesting period, fertilizer recovery efficiency, fertilizer dosage, and spatial layout of the overall land use planning were obtained from environmental and agricultural management departments or collected by current questionnaire survey.

SWAT is mostly used to evaluate N and P pollutants production, diffusion and movement, and transformation. These pollutions whole process control occur simultaneously with the soil

erosion, hydrological cycle and reasonable utilization of land resource. SWAT considers 5 forms of N and 6 forms of P. The N and P cycles contain mineralization, decomposition, solidification/stabilization, and conversion. The NPS pollutant loading function is the basis for evaluating N and P distribution, transportation and transformation (Zhang, 2005). Organic N and P loss was calculated by SWAT by the comprehensive evaluation model of the NPS pollutant loading, variations of nutrient elements and salt contents of soil, soil environment, crop growth, and crop yield. The total amount of nitrate lost in the soil was calculated by the multiplication of water volume and nitrate concentration in the water. Water volume consisted of groundwater runoff, surface runoff, and interflow/subsurface flow/groundwater recession flow. The soluble P removed in the runoff was estimated using the P concentration in the soil partitioning coefficient, surface soil layer, and runoff volume. The concentration of soluble P in the water was calculated by topsoil P stocks, runoff variation and influencing factors, soluble P ratio, and soil particle-size characteristics.

Surface runoff from daily rainfall data and land use in HRU/sub-basin were calculated and evaluated using the SCS-CN method. Using the SCS-CN curve, vertical distribution characteristics and temporal stability of soil water, runoff module number of the ground water, Soil saturated water content movement and hydraulic conductivity were determined, as well as the related parameters for daily rainfall. The total discharge temporal variations of runoff from sub-basin/HRUs is the dynamic equilibrium of groundwater runoff flow, surface runoff flow, and interflow/subsurface flow. The main routes for water cycle simulation in the SWAT follow either the network-node mode or the natural-artificial dualistic water cycle mode in river basins under changing conditions. We used the dualistic mode SWAT flow varies with the dynamic changes in infiltration, evaporation, transport, and nutrient cycling (Arnold et al.,1998). Direct

runoff is surface runoff resulting from rainfall, which includes surface and return flows. Baseflow is part of the groundwater recharge to river runoff. Most of the base flow and direct runoff separation methods are performed by mathematical methods. We used Digital-Filter-Equation to divide the base flow:

$$\begin{cases} q_t = \beta . q_{t-1} + \alpha(1+\beta)(Q_t - Q_{t-1}) \\ b_t = Q_t - q_t \end{cases} \quad (1)$$

Here, q_t is the surface runoff at time t; Q_t is the total runoff at time t; b_t is the base flow at time t; and α β are filter parameters.

Digital filtering is an objective and effective method of base-stream separation. We assigned α =0.5 and β =0.925 in the HTRW (Arnold & Allen,1999). The SWAT HRUs used the soil and water loss factors, hydrodynamic process of soil erosion, and the universal soil loss equation (MUSLE) to analyse erosion and sediment form, space distribution characteristic and influencing factor (Williams, 1975). Sediment was routed through channels using Bagnold's sediment transport equation (Bagnold, 1977). We used a 2009 version of SWAT to calculate the parameters.

2.3.2. Model data input

DEM, underlying surface status, geomorphology, soil properties, land vegetation, hydrological and meteorological data (rainfall, evaporation, temperature) were imported into the SWAT (Niraula et al.,2013). Fig. 3 shows the basic data used in the SWAT model. We used 30×30 grid data (elevation) as the basis for DEM operation. We downloaded the DEM data for the HTRW location from the SRTM (Shuttle Radar Topography Mission) data pack. These free data can be obtained from the website, http://srtm.csi.cgiar.org/SELECTION/inputCoord.asp. The DEM was used to extract the study area and analysis the stream network structure in relation to geomorphologic features. The stream network in the HTRW was extracted using

1:250,000 digital water system data (www.geodata.com) as an auxiliary model to construct the HTRW stream network model. We delineated land-use types into 27 categories. The main type of HTRW land use and land cover change is forest (including orchard, 49%), dry land (24%), rice paddy (15%), urban land (vacant land, 8%), unused land (uncultivated land, 3%) and grassland (1%). Soil types were classified into 26 types. The primary soil types are brown soil (54%), meadow soil (30%) and paddy soil (11%). The underlying substrate database was constructed based on the soil type database using the soil properties and land development data as underlying substrate parameters (topography characteristics, surface vegetation and soil types and distribution characteristics). The soil parameters were got from national earth system science data sharing infrastructure database (http://www.geodata.cn/aboutus.html). The watershed meteorological data used in the current research include rainfall data for 1990-2009 collected by 76 rainfall stations/hydrometric network and hydrometeorological data for 1990-2009 obtained by 12 city meteorological stations. The missing meteorological information can be estimated using the Long Ashton Research Station Weather Generator (LARSWG-5). At least 3 sets of water monthly monitoring data for ammonia (such as NH_3 and NH_4), nitrite (NO_2), nitrate (NO_3), TP, and TN, were available for 2006–2009. We obtained information on plant species, cropping systems, sowing time, fertilization time, distribution pattern of soil productivity, and regional economic-social development from investigations and the statistics department in HTRW. The SWAT uses the LH-OAT (Latin Hypercube One-factor-At-a-Time) sensitivity analysis method and the SCE-UA (Shuffled Complex Evolution Algorithm) automatic calibration analysis method to determine the value of sensitive parameters.

Data information (scale, type, description) for SWAT in the HTRW are shown in Fig. 3. We imported the related soil and meteorological data for SWAT from the China Meteorological

Administration and Environmental-Ecological Science Data Center for West China. The China Hydrology, Water Resources and Water Quality Monitoring Department of the HTRW provided the automatic and regular monitoring hydrological data sequence. The Liaoning Province Water Resources Administrative Bureau granted permission for the modelling the pollutant generation response to different land utilization scenarios in the HTRW.

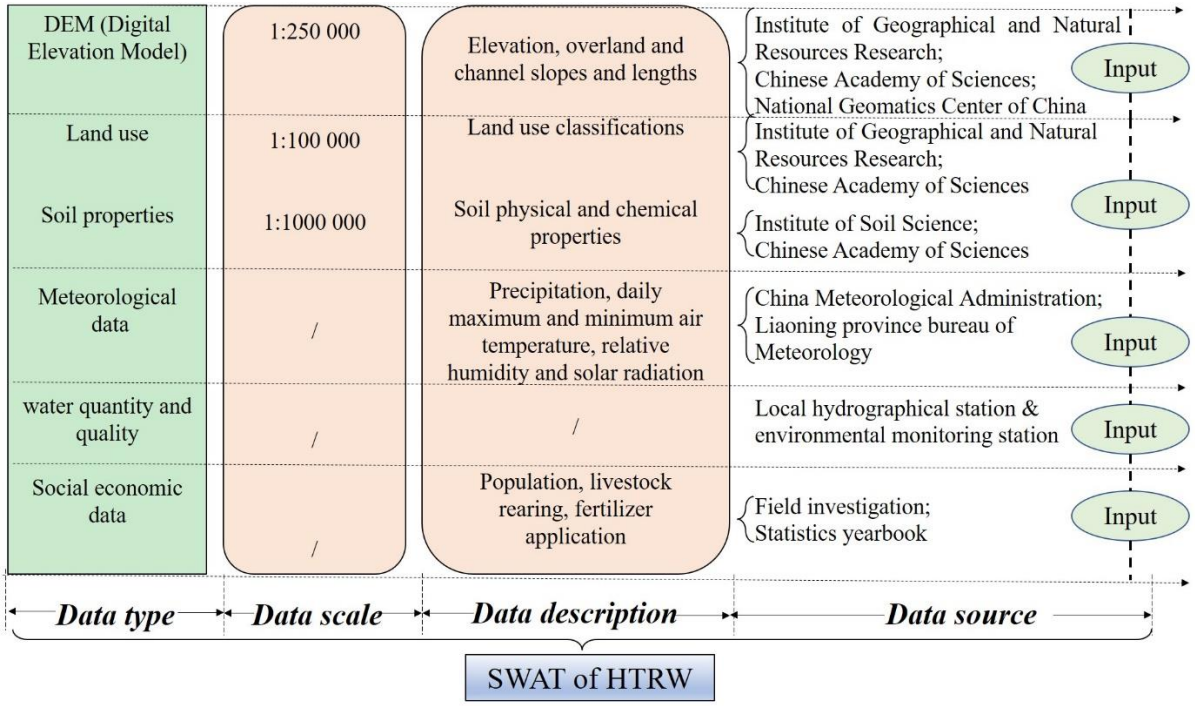

Fig. 3. HTRW data. The basic data imported into the SWAT model included spatial data and attribute data. Spatial data includes DEM, land use and land cover data, soil spatial distribution data, digital river network data, and the spatial location of meteorological stations and hydrological stations. Attribute data mainly includes land use attribute database, soil type attribute database, LARSWG-5 and hydro-meteorological data.

2.3.3. Calibration and validation

The monthly scale data were used to simulate SWAT. We used the open code SWAT-CUP module to calibrate the parameters of SWAT in HTRW (Abbaspour et al.,2007). A sequential uncertainty fitting algorithm had a higher calculation accuracy and efficiency, which was

extensively used in the SWAT-CUP module (Wang et al.,2014; Yang et al.,2008). We manually input the optimal parameters into the SWAT model for hydrology series simulation. The E_{NS} (Nash-Sutcliffe efficiency coefficient), *Dv* (relative deviation), and R^2 (certainty coefficient) were used to assess the runoff flow change of the HTRW hydrological station.

The runoff was calibrated, followed by N, P and other nutrients. The runoff was calibrated and tested using monitoring data from the Xingjiawopeng and Tangmazai hydrological stations (Fig. 2). The simulated values of N and P were calibrated using on-site monitoring data from Dongling bridge, Beikouqian, Xiaolinzi, Xingjiawopeng, and Tangmazhai hydrological stations. We automatically calibrated 10 sensitivity parameters, then we applied the SWAT manual calibration helper to make small and targeted adjustments to the calibration results to improve the simulation accuracy based on auto-calibration results. Various water quality and hydrologic parameters (test data) were adjusted under their change interval to fit with the monitored/observed data (Fig. 4). GWQMN, SURLAG, and ESCO were three key parameters in the calibration and water flow validation (Shen et al., 2010). The other sensitive parameters selected for calibration and validation in the HTRW are shown in Fig. 4. In the HTRW, the Liaoning Province government began monthly monitoring of pollutants in 2006. The TN and TP loading, and runoff data, used for calibration and validation were from 1992 to 2009 and from 2006 to 2008, respectively.

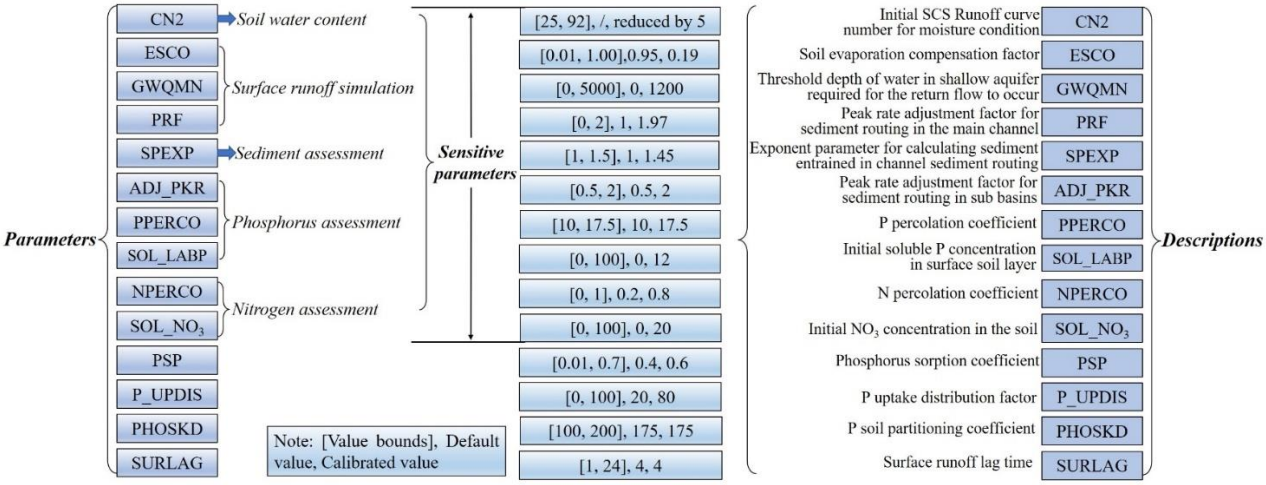

Fig. 4. Parameter values of SWAT model in the HTRW. Based on the spatial analysis of sensitive parameters, we analyzed the influencing factors of the parameter values combining with the underlying surface runoff factors of the basin.

In the present study, the simulated effects were evaluated by analyzing and comparing the runoff hydrograph, *Dv*, E_{NS} and R^2. The *Dv* was used to simulate the entire water quantity deviation; E_{NS} and R^2 were used to simulate the simulation effects (Nash, 1970). The *Dv*, E_{NS} and R^2 were calculated as

$$D_v = [(M - W)/W] \times 100\% \quad (2)$$

Here, D_v was the relative deviation; W was the observed mean value; and M was the predicted mean value.

$$E_{NS} = 1 - [\sum_{i=1}^{n}(W_i - M_i)^2 / \sum_{i=1}^{n}(W_i - \overline{W})^2] \quad (3)$$

Here, E_{NS} was the Nash-Sutcliffe efficiency coefficient; W_i was the observed data at the i^{th} period; M_i was the simulated data at the i^{th} period; and $\overline{W}$ was the observed mean value.

$$R^2 = \{[\sum_{i=1}^{n}\left(W_i - \overline{W}\right)\left(M_i - \overline{M}\right)]/[\sqrt{\sum_{i=1}^{n}\left(W_i - \overline{W}\right)^2}\sqrt{\sum_{i=1}^{n}\left(M_i - \overline{M}\right)^2}]\}^2 \quad (4)$$

Here, R^2 was the certainty coefficient; W_i was the observed value at time i; M_i was the simulated

value at time *i*; $\overline{W}$ was the observed mean value, and $\overline{M}$ was the predicted mean value.

The first four years (1990-1994) were regarded as the stage for SWAT to minimize the uncertainty of initial meteorology and underlying surface values. Sensitivity analysis of the parameters is an effective mean to help assessing impact of uncertainty in the input and parameters on the output uncertainty. The sensitivity evaluation indicators differed between SWAT and SWAT-CUP. Student's t-test is used by SWAT-CUP and is part-sensitive. To improve the model calibration accuracy and verification results, we used SWAT-CUP and the SUFI-2 algorithm to analyse the parameters' sensitivity. To determine the sensitivity of various parameters, one parameter was auto-adjusted at a time based on the accuracy and change interval in Fig. 4. To calibrate the stream flow, we subsequently calibrated runoff and nutrients (TP and TN) with the same geographical and hydrological data. During calibration, we used R^2 and the correlation coefficient of the residual sequence (*SCR*) to eliminate the uncertainties caused by the differences in water quality sampling and testing methods.

3. Results and discussion

3.1 Modelling validation

Stream flow. Because of HTRW lacks basic runoff data, the present study focused on calibrating and testing the runoff model. First, we dealt with the meteorological data and retained the 1990-2001 data series, then supplied the meteorological data simulation value from 1990 to 2001 by SWAT. Second, we input the runoff data for 1995-2001 into the SWAT-CUP model to calibrate the runoff parameters and entered these parameters into the SWAT database, then extended the meteorological data series to 1990-2009 and simulated runoff again. Finally, we compared the runoff simulation values with monitoring values from 2002 to 2009. During

343 annual calibration, the runoff curve data were calibrated and the available water content in the
344 soil and the soil evaporation compensation coefficient were modified. Finally, the monthly
345 runoff curve was modified. CN2 is a comprehensive parameter that reflects the watershed
346 characteristics before rainfall and is mainly affected by the hydrology and soil types, land use,
347 pre-soil moisture and tillage management measures. CN2 directly affects the surface runoff,
348 and the larger the CN2 value, the larger the runoff yield. The same land-use type yields greater
349 permeability with a smaller CN2 value or lower vegetation coverage and rainfall interception
350 ability with a greater CN2 value. Different HRUs have different CN2 values. The moist area
351 (climate division) has the highest CN2 ranging from 60~96, while other regions vary greatly.
352 Within the same soil types, the CN2 value was the highest for cultivated land, followed by
353 grassland. Woodland was the lowest. For the simulation, 1990-1994 was the model preparation
354 period, 1995-2001 was the model calibration period, and 2002-2009 was the model validation
355 period. There are 6 samples of each site. Samples were obtained during the wet season, the wet
356 season, intermediate season, and dry season. Two samples are set for each water period.

357 For the calibration step, E_{NS} and R^2 for Xingjiawopeng hydrological station and Tangmazhai
358 hydrological station were both greater than 0.6, and the $|Dv|$ values were less than 20% during
359 the model preparation period, suggesting that the SWAT model parameters were reliable after
360 calibration. The monitoring value fit better with the simulation value obtained from
361 hydrographic curve. Most top values observed were highly similar. For the model calibration
362 period, the matching curves for the simulated and measured monthly runoff values at
363 Xingjiawopeng and Tangmazhai hydrological stations are shown in Figs. 5(a) and (b). The
364 runoffs at these two hydrological stations were well matched. However, the accuracy of the
365 simulated runoff for the second halves of the years 2002, 2005 and 2006 was poor, likely due

to the data series length and specific stations selected. For the simulation and evaluation standards for the hydrological model, the simulation effects at the monthly scale were much better.

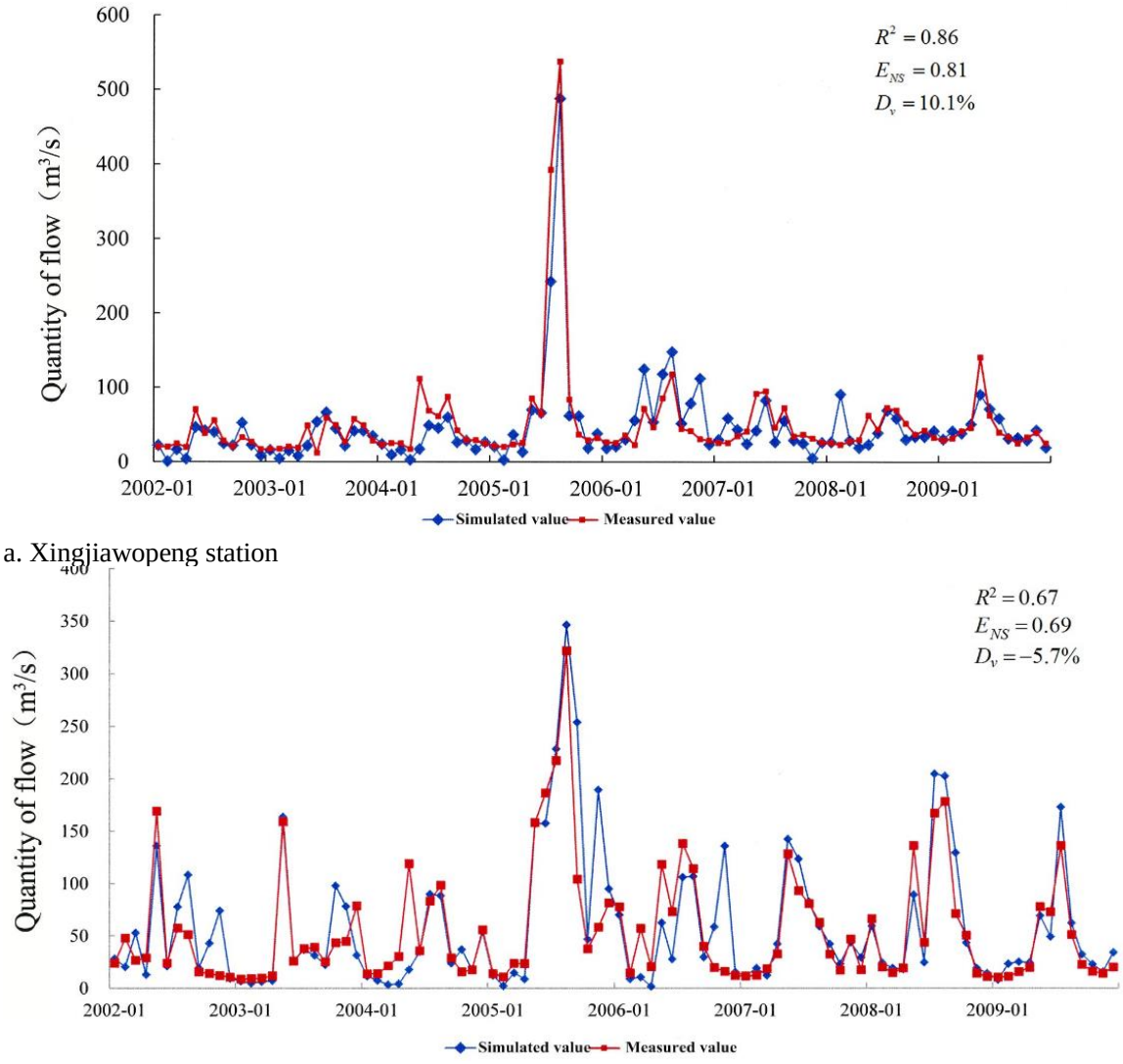

a. Xingjiawopeng station

b. Tangmazhai station

Fig. 5. Stream flow validation of a typical monitoring station.

Nutrients. The nutrient concentrations in the water were simulated by SWAT. By verifying the accuracy of the initial concentrations, the nitrate and soluble P loading can be simulated by adjusting the nitrogen permeability coefficient (NPERCO) and the phosphorous permeability coefficient (Lam et al., 2011). Beikouqian, Xingjiawopeng, Xiaolinzi and Tangmazhai

hydrological stations had continuous monthly water quality monitoring data from 2006 to 2007 (model calibration period). Only the monthly data on TN and TP in Beikouqian were validated from 2008 to 2009. The Xingjiawopeng, Xiaolinzi and Tangmazhai Hydrological stations had only the TN data during the study period; therefore, Beikouqian was selected for the validation curves, and the TN E_{NS} and R^2 were 0.64 and 0.78, and the TP E_{NS} and R^2 were 0.60 and 0.75, respectively (Figs. 6 a and b). The E_{NS} and R^2 for the Xingjiawopeng, Xiaolinzi and Tangmazhai hydrological stations were 0.62 and 0.73, 0.61 and 0.72, and 0.62 and 0.77, respectively. The values of all R^2 were higher than 0.7, confirming that the SWAT could be used for water quality simulation in HTRW. The simulated TN and TP have a certain synchronization with the measured changes of TN and TP in each month. The variation law of simulated N and P content is not much different from the measured value, and the model has good workability.

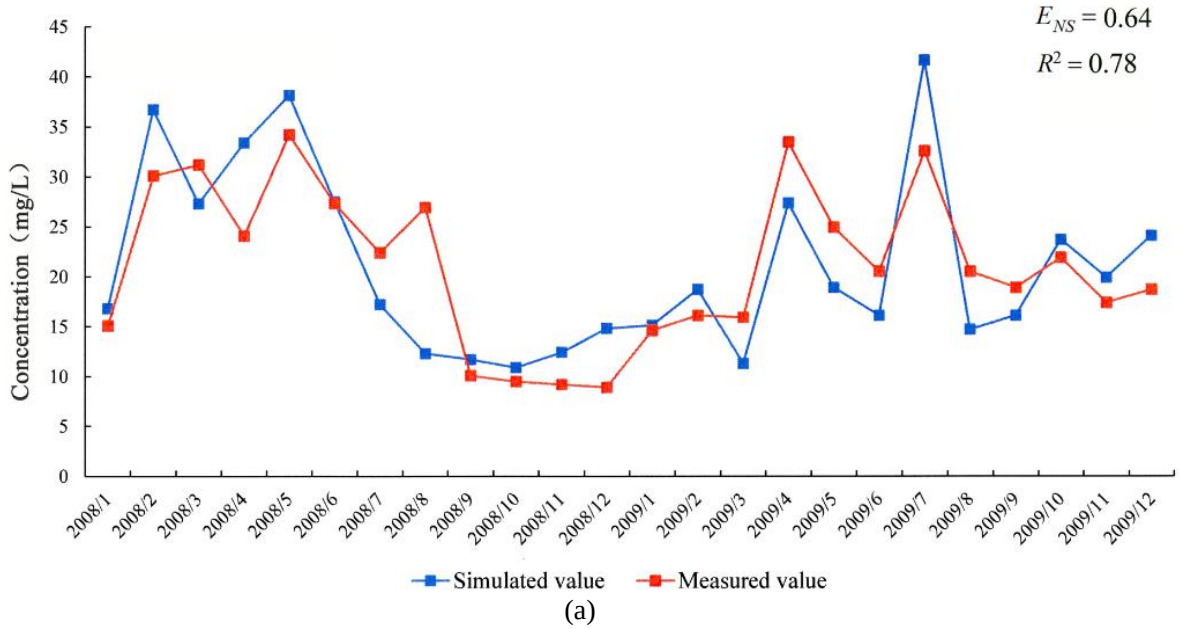

(a)

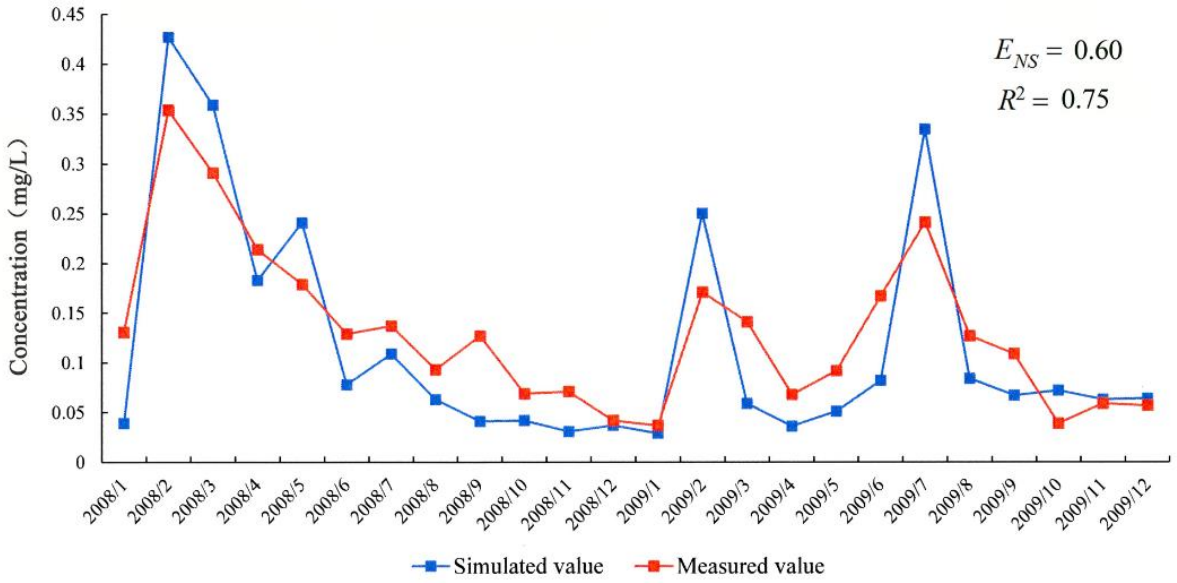

(b)

Fig. 6. Nutrient validation at Beikouqian station. Figure (a) and (b) shows the fitting result of TN and TP, respectively.

3.2 NPS pollutant loading under the status quo scenario

The NPS pollutant generation output was calculated using the pollutant loading approach based on the attributes of the regional calculation results and land-use scenarios in HTRW. The generated N and P for different calculation units were calculated based on the spatial changes in soil types, crops and residuals, as well as the differences in the coefficients of N and P losses under different land uses. The paddy fields, rural residential areas, urban development, and vegetation type may be important indicators for variability in NPS pollution, and nutrition pollution was influenced by the integrated effects of different land uses (Cai et al., 2015; Lee et al.,2010). The annual generated TN and TP were 18,707 t and 53,322 t, respectively (Table 1). Brown soil is widely distributed in the HTRW. We supplied the N and P loss characteristics under different land-use types and fertilization, as shown in Table 2 (Hao, 2012). The brown soil thickness was 30-50 cm in HTRW. The organic content, TN and TP

399 decreased significantly with the soil depth increment. Nutrients were mainly found in soils
400 of 0-30 cm deep, where TN and TP reserves reached more than 50% of the total soil reserves.
401 Large-scale use of fertilizers (DAP, N:46.4% and N-P-K, N:15%; P_2O_5:15%; K_2O:15%) and
402 livestock and poultry excrement (N:0.5-0.6%; P:0.45-0.6%; K:0.35-0.5%) were the important
403 sources of agricultural NPS pollution. In HTRW, the number of pastures and cattle was small,
404 and cattle excrement was collected and processed by the farmer. The excessive or unreasonable
405 application of fertilizers and the fertilizer utilization rate were not high (the utilization rate of
406 nitrogen is 30% to 60% and of phosphorus is 2% to 25%), resulting in substantial fertilizer loss.
407 The nutrient content (mainly from agricultural production activities) of the soil (20cm below
408 the surface) in the HTRW was 1.21 t/ha. Information on initial soil nutrient content and
409 fertilizers was used for model parameterization.

410 **Table 1.** Pollutant generation in the HTRW under the status quo scenario

Watershed	Area (km^2)	Run off (E+08 m^3)	Pollutant (t)			Pollutant loading (kg/ha)		
			Sediment	TP	TN	Sediment	TP	TN
Hunhe River	11,565	24.04	220,004	8,993	24,264	190	8	21
Taizi River	13,903	33.31	1,699,996	6,399	19,010	1,223	5	14
Daliao River	1,913	1.60	300,002	3,315	10,048	1,568	17	53
Total/Average	27,381	58.95	2,220,002	18,707	53,322	811	7	19

411 Source: China Hydrology; national earth system data sharing infrastructure; field investigation of Liaoning
412 province; chemical fertilizer/land area/soil erosion statistics yearbook of Liaoning province; Liaoning
413 province Bureau of Meteorology.

414 **Table 2.** Loss characteristics of N and P under different land uses and fertilization

Land use	Soil thickness (cm)	Organic matter content (g/kg)	Unit weight of soil (g/cm^3)	Soil particle composition (mm)			TN (g/kg)	TP (g/kg)
				Clay ø≤0.002	Loam 0.002<ø≤0.005	Sand 0.005<ø≤2		
Cultivated field	0-5	24.58	1.42	21.05	57.35	21.6	0.96	0.47
	5-30	18.45	1.48	24.71	24.71	18.84	0.88	0.38
Grassland	0-5	27.6	1.18	15.97	15.97	14.58	1.25	0.58

5-30	21.75	1.25	20.36	20.36	21.5	1.02	0.42

3.2.1. Sediment

Sediment loading is the data basis for calculating TN and TP loading and is affected by the type of land development and vegetation coverage (generally dominated by forest and farmland). Based on the SWAT model simulation, the annual sediment outputs generated in the Hunhe, Taizi and Daliao River watersheds were 22×10^4 t, 170×10^4 t and 30×10^4 t, respectively. The annual soil erosion loading in HTRW was 0.811 t/ha, and its spatial distribution is shown in Fig. 7(a). The soil erosion value varied widely in different regions, with the change interval from 0 to 2 t/ha. Soil erosion in the Daliao River watershed was severe (up to 2 t/ha in some regions), followed by the Taizi River watershed (1 t/ha in most regions) and the Hunhe River watershed (less than 0.2 t/ha in most regions). Yingkou and Dashiqiao have even topography, and incoming silt from the upper areas is accumulated therein. The soil erosion modulus is therefore very high, which contributes greatly to the silt input to the HTRW. The soil erosion was affected by natural and human factors. The natural factors mainly included topography, underlying surface conditions and soil type. The human factors mainly consisted of vegetation coverage, precipitation, land use, crop cultivation and cultivated land farming methods. Moreover, mountainous areas have great soil erosion (Hong et al.,2012). The Daliao River had a large cultivated land area; therefore, soil erosion was more likely. Soil types are also key influencing factors in causing soil erosion; therefore, brown and paddy soils are prone to accumulating sediment (Hong et al.,2012).

3.2.2. TP

From the SWAT simulation results, the annual TP output generated in the Hunhe, Taizi and Daliao River watersheds was 8993 t, 6399 t and 3315 t, respectively, and the HTRW output

loading was 7 kg/ha. The TP loading had the same spatial distribution pattern as the sediment loading, ranging from 0 to 260 kg/ha. Fig. 7(b) shows the TP spatial variation loading of the HTRW. A large amount of P could be deposited in the downstream plain. The changes in the TP loading were affected by topography, precipitation, land use, and silt losses. The TP output loading on the Daliao River watershed slope was higher than that of the Hunhe River watershed, while the Taizi River watershed was the lowest. Many fertilizers and pesticides have been applied to the farmland, and organophosphate pesticides accounted for 40% of the total pesticides (Wang, 2012). The paddy fields, brown soil and dry lands were mainly distributed in the Hunhe River downstream. Therefore, the P loading in these plains areas was higher (Li et al., 2010). Correspondingly, the cities and counties with large proportions of farmland have higher TP output loading, such as Dashiqiao, Panshan and Dawa city in the Daliao River watershed and the city of Haicheng and Taian county in the Hunhe River watershed. Regions with large proportions of developed land have lower TP output loading, including the city centre of Fushun, Shenyang in the Hunhe River watershed, the municipal districts of Liaoyang city and Benxi city at the Taizi River watershed. Based on land use, tributaries with higher proportions of farmland have the highest TP output loading, while tributaries with substantial vegetation cover as forested land have relatively lower TP output loading. TP output loading is closely related to soil characteristics and attributes. The buffer zone was only 1km wide and the vegetation on both sides of the river grew slowly. HTRW is located in the northeastern of China and which has long and cold winter. From October to April, the vegetation in the buffer zone is almost withered. Therefore, the average removal rate of the buffer zone to TP is 10%. Although the data is not high, it reflects the impact of regional and climatic conditions on TP removal.

3.2.3. TN

Simulation and calculation results showed that the TN generation output in the Hunhe, Taizi and Daliao River watersheds was 24264 t, 19010 t and 10048 t. The annual TN output loading in the watershed was 19 kg/ha. Fig. 7(c) shows the spatial variation of TN loading in the HTRW. The TN loading interval varied from 0.001 to 365 kg/ha. The TN loading had the same spatial characteristics as TP loading. The TN output loading in the Daliao River watershed was greater than that in the Hunhe River watershed, while the Taizi River watershed was the lowest. Large amounts of fertilizer were applied in the study area. Nitrate and organic N accounted for a substantial portion of the fertilizer used in HTRW. Therefore, the TN output loading in the watershed was very high. Regions with much farmland, such as the middle and lower portions of the Hunhe River, the lower portions of the Taizi River and the tributaries in the upper portions of the Daliao River, have high TN output loading. The organic N contents in the forested land were very low. Thus, the output loading of TN in regions with high vegetation forest cover, such as the mountainous areas in the upper parts of the Taizi and Hunhe rivers, was very low. The TN output loading in municipal districts with highly developed areas was the lowest, such as in the municipal districts of Fushun city and Shenyang city in the Hunhe River watershed and the municipal districts of Benxi city, Liaoyang city and Shenyang city in the Taizi River watershed.

TN and TP loading in the HTRW were characterized by a regional distribution. Although Qingyuan, Yibin and Benxi counties, located in the upper areas of the HTRW, had high water and silt output, their pollutant loading was low. Per unit area, the maximum TN and TP loading (maximized over space) was 365 and 260 kg/ha, respectively. The regions TN and TP with high loading were mainly distributed in Taian, Haicheng, and Fushun city. The TP and TN loading

near the Dahuofang, Tanghe, Shenwo and Tanghe reservoirs were low, ranging from 0.006 to 10 kg/ha and from 0.08 to 19 kg/ha, respectively. Based on topography and soil distribution, the slope is very steep in the upper stream of HTRW. The soils are predominately brown soil and salted paddy soil, both of which are easily eroded. The topography in the lower sections is usually flat, such as in the cities of Anshan, Haicheng, Yingkou and Panjin. The elevation is low, and the soil is predominately meadow soil and brown soil, both of which have higher soil erosion rates, silt loss and output loading of pollutants. The regions with heavy TN and TP loading included Xinmin county, located in the middle and lower reaches of the HTRW, the municipal district of Shenyang city, Liaozhong county, Dengta city, Liaoyang county, the municipal district of Anshan city, Haicheng city and a portion of Dashiqiao city. Based on the land development pattern in the Taizi River, dry fields and paddy fields were mainly distributed on the plain areas of this watershed, which constitute therefore a core source of output loading. The spatial differences in the TN and TP loading were no large differences. Based on topography, landform, soil types and land development status in the watershed, the upper streams of the watershed have high vegetation coverage, less farmland and low pollutant loading, while the lower areas have more farmland, high fertilizer application rates and high soil erosion and pollution loading (Yin et al.,2011). In summary, the spatial characteristics of TN loading resulted from comprehensive effects of precipitation/runoff characteristics, soil properties, soil erosion and vegetation coverage. Therefore, to effectively control TN loading and soil erosion in the HTRW, the BMPs, fallow measures of cultivated fields, watershed vegetation restoration and soil and water conservation in the upper stream are the most important measures to implement.

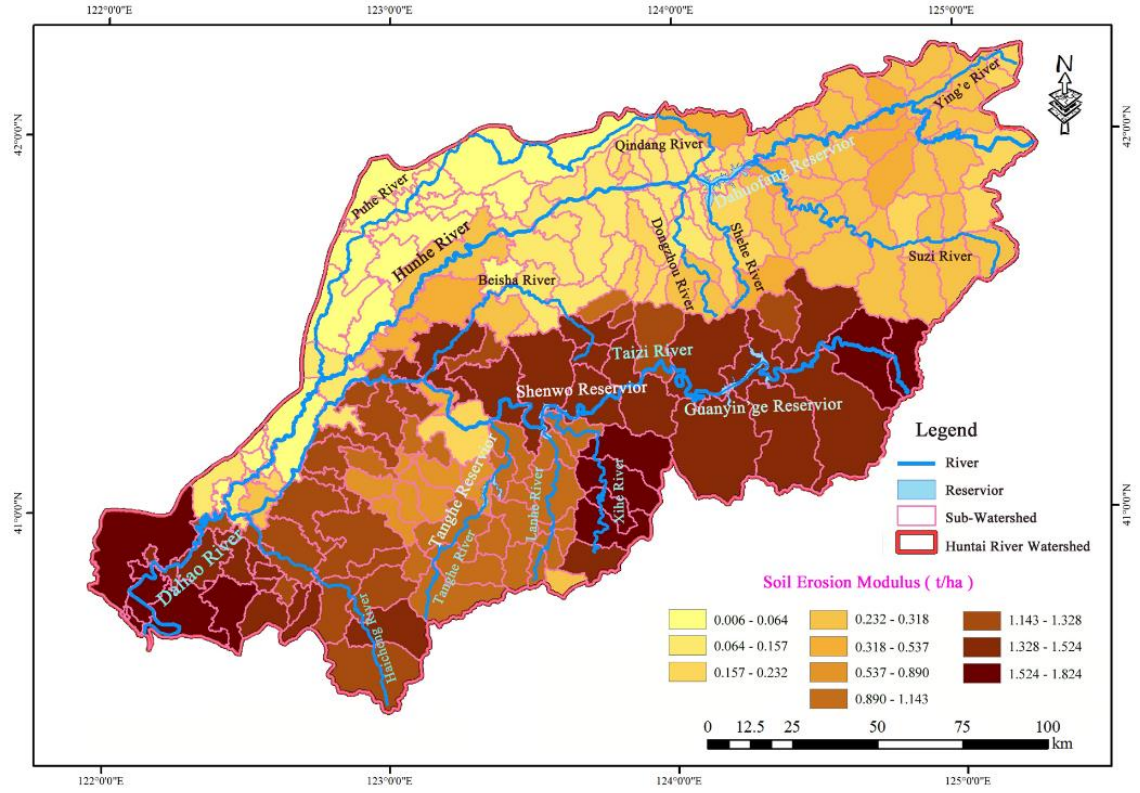
122°0'0"E
123°0'0"E
124°0'0"E
125°0'0"E
42°0'0"N
41°0'0"N
N
Ying'e River
Qindang River
Dahuofang Reservior
Puhe River
Hunhe River
Beisha River
Dongzhou River
Shehe River
Suzi River
Taizi River
Shenwo Reservior
Guanyin'ge Reservior
Xihe River
Lanhe River
Tanghe Reservior
Tanghe River
Daliao River
Hunhe River
Legend
River
Reservior
Sub-Watershed
Huntai River Watershed
Soil Erosion Modulus (t/ha)
0.006 - 0.064
0.064 - 0.157
0.157 - 0.232
0.232 - 0.318
0.318 - 0.537
0.537 - 0.890
0.890 - 1.143
1.143 - 1.328
1.328 - 1.524
1.524 - 1.824
0 12.5 25 50 75 100
km

(a)

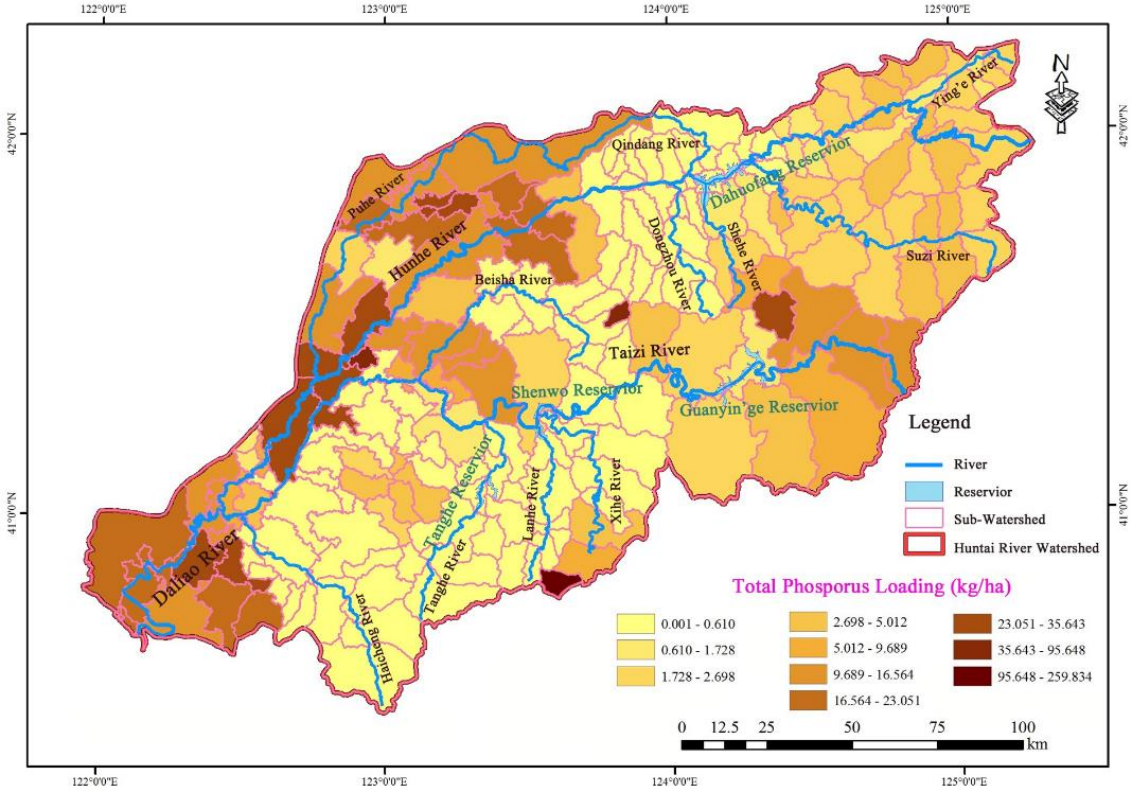
122°0'0"E
123°0'0"E
124°0'0"E
125°0'0"E
42°0'0"N
41°0'0"N
N
Ying'e River
Qindang River
Dahuofang Reservior
Puhe River
Hunhe River
Beisha River
Dongzhou River
Shehe River
Suzi River
Taizi River
Shenwo Reservior
Guanyin'ge Reservior
Xihe River
Lanhe River
Tanghe Reservior
Tanghe River
Daliao River
Hunhe River
Legend
River
Reservior
Sub-Watershed
Huntai River Watershed
Total Phosporus Loading (kg/ha)
0.001 - 0.610
0.610 - 1.728
1.728 - 2.698
2.698 - 5.012
5.012 - 9.689
9.689 - 16.564
16.564 - 23.051
23.051 - 35.643
35.643 - 95.648
95.648 - 259.834
0 12.5 25 50 75 100
km

(b)

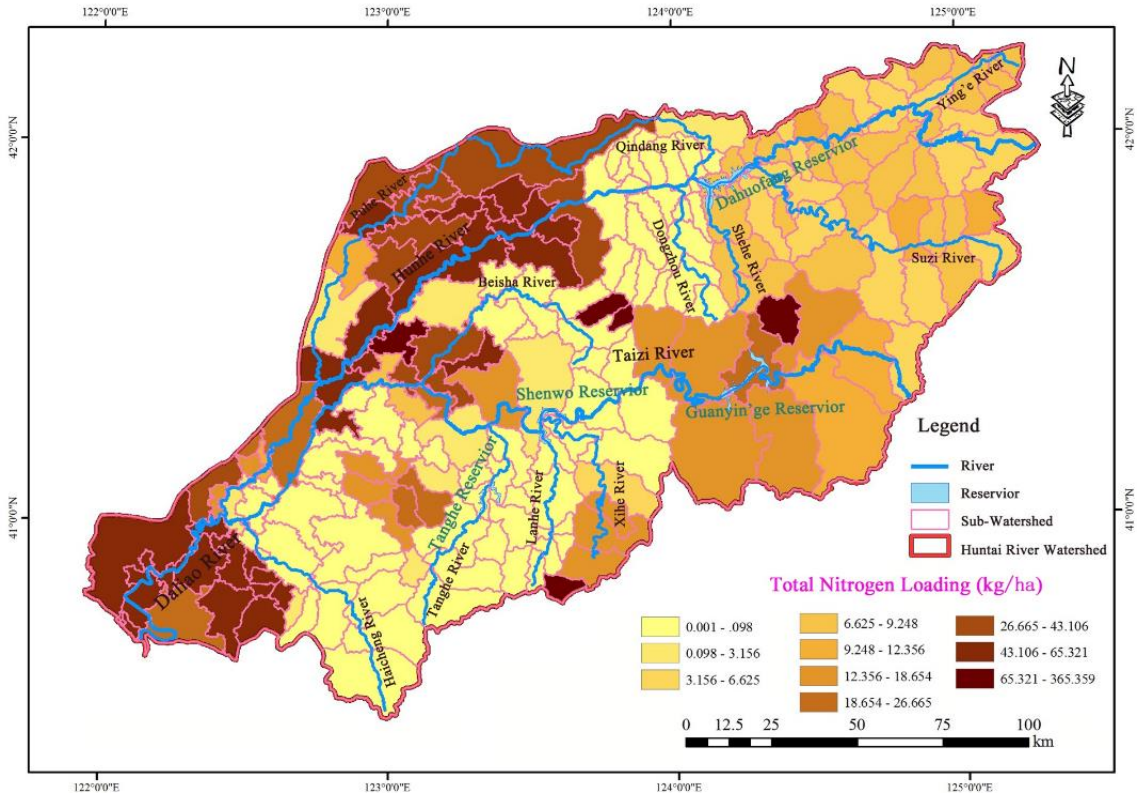

(c)

Fig. 7. NPS pollution loading distributions of HTRW under the status quo scenario. The Figure (a), (b) and (c) showed the loading distributions of contaminant sediment, TN and TP, respectively.

3.3 NPS pollutant loading under EPS

There exists a correlation between land development mode and water environment protection and rehabilitation at the basin scale. The riparian buffer zones effectively reduced the concentration levels of NO_3^- in the water, which were 47% lower than those of the soil content. Dry farmland caused higher NPS pollutant loading, followed by paddy lands, rural and urban areas, forestland, and shrub lands. Hence, under the EPS, the farmland area in the watershed was reduced. A modest area of farmland (29,500 ha, accounting for 3% of the total farmland area) was converted to forestland (including shrub land, 14,753 ha; grassland, 5,899 ha; and wetland, 8,848 ha), while NPS pollution from farmland decreased. The water quality

protection objective within the watershed's critical zoning was realized. The riparian buffers can be planted in various diverse vegetations. The N removal rate of a 60-m-wide woody soil buffer zone was 16% and 38% higher than that of shrubbery and grassland, respectively. Approximately 1 kilometre within both banks of the Hunhe, Taizi and Daliao river tributaries and 5 kilometres of surrounding reservoirs buffer zones were defined, including 1946 km^2 of farmland, urban land, and rural residential land. This accounts for 7% of the total area in the watershed. The woodland coverage rate was reduced by 1%, and the loading of sediment, TP and TN increased by 0.01-11, 0.2-3 and 0.4-14 kg/km^2, respectively. The pollutant generation output under EPS was calculated by transforming the existing land-use type.

The TN and TP respective ranges of change were 0 to 365 kg/ha and 0 to 260 kg/ha. The annual losses of TN and TP were reduced by 13,839 and 1,946 t/yr., respectively. In comparison, the NPS pollutant generation output under the EPS was decreased by 22% compared with that under the SQS, whereas the TP and TN outputs were reduced by 10% and 26%, respectively. Under the EPS, the average loading of TN and TP was 14 and 6 kg/ha on a unit area basis, which were 14% and 26% less than the loading under the SQS, respectively. The NPS pollutant loading declined in the EPS. The variation of TP and TN pollutant loading between the SQS and EPS is shown in Table 3. The amount of change indicated that riparian buffer and land development pattern change effectively reduced NPS pollutant loading in the HTRW.

Table 3. Loading variation in TP and TN pollutant between EPS and the status quo scenario

Watershed	Pollutant loading of EPS (kg/ha)		Pollutant loading variation (kg/ha)		Farmland variation (ha)	Forestland variation (ha)	Grassland variation (ha)	Wetland variation (ha)	Pollutant annual variation(t/yr.)	
	TP	TN	TP	TN					TP	TN
Hunhe River	7	16	-1	-5	-12,460	+6,231	+2,492	+3,737	-838	-5,743
Taizi River	4	10	-1	-4	-14,979	+7,491	+2,995	+4,493	-776	-5,606
Daliao River	16	40	-1	-13	-2,061	+1,031	+412	+618	-332	-2,490
Total/Average	6	14	-1	-5	-29,500	+14,753	+5,899	+8,848	-1,946	-13,839

"—" denotes a decrease compared to that of the status quo scenario; "+" denotes an increase compared to

that of the status quo scenario.

3.4 Value transformation based on NPS pollutant loading

Based on the results of Simpson (2014), the correlation between the yield, input of land, purchase investment, ecosystem services value, and land area is expressed as

$$q = f(x, S, A) \tag{6}$$

where q is the yield, x is the quantity of the purchase investment, S is the quantity of the supplied ecosystem services, A is the land area directly utilized for agricultural production. Formula (6) is a conceptual formula, and there is no sole unit for each letter in formula (6).

To obtain a general expression, we give a special instance of production function.

$$q = f(x, S, A) = x^{\alpha} S^{1-\alpha} - \gamma (x^{\alpha} S^{1-\alpha})^2 / A \tag{7}$$

Where α=1/2, γ was a positive constant.

The constant profit of a massive production function is expressed as (Vincent & Binkley, 1993)

$$q = \sqrt{x \cdot S} - \gamma \cdot x \cdot S / A \tag{8}$$

This is a simple production function with limitations. Assuming that r represents the price of the input. When the price of the yield is normalized as 1, the profit η is expressed as

$$\eta = \sqrt{x \cdot S} - \gamma \cdot x \cdot S / A - r \cdot x \tag{9}$$

For x, the first-order condition for maximal profit is expressed as

$$\begin{cases} \frac{1}{2}\sqrt{S / x} - \gamma \cdot S / A - r = 0 \\ -\frac{\varphi}{2}\sqrt{x / S} + \gamma \cdot x \cdot \frac{\varphi \cdot \bar{A}}{A^2} = 0 \end{cases} \tag{10}$$

and when the first-order of Eq. (10) is satisfied, the second-order condition for maximal management was also satisfied. After the conversion, we obtained

$$x = \frac{S}{4(\gamma \cdot S / A + r)^2} \qquad A = \frac{\overline{A}}{1 + \sqrt{r / \gamma \cdot \varphi}} \tag{11}$$

The ecosystem services of the preserved land were determined by the parameter, φ. In the production function, ecosystem services and the purchase investment were the substitute items. When the purchase price increases, the area of the land used for production will decrease, suggesting that more land should be preserved. When more land is preserved for maximal profit, the yield will decrease. When Eq. (10) was multiplied by x, we obtained

$$\frac{1}{2}\sqrt{x \cdot S} - \gamma \cdot x \cdot S / A - r \cdot x = \eta - \frac{1}{2}\sqrt{x \cdot S} = 0 \tag{12}$$

where the total differential of Eq. (12) was calculated concerning A. If A and x were used to realize maximal profits, the arithmetic resolution could be calculated as

$$\frac{\mathrm{d}x / x}{\mathrm{d}A / A} = \frac{A}{\overline{A} - A} \tag{13}$$

therefore, when most of the land was used for production, the dependence on the purchase investment increased. If more land was used in agricultural production activities, greater costs would be paid to compensate for lost ecosystem services. If the initial consideration was the excessive dependence on purchase investments, the margin rate of technically replacing the purchase investment by ecosystem services increased, indicating that the purchase investment would be reduced significantly.

If the land area used for agricultural production was changed, profits ($\partial q/\partial x=r$) were maximized by

$$\frac{\mathrm{d}q / q}{\mathrm{d}A / A} = \frac{r \cdot x}{q} \frac{A}{\overline{A} - A} \tag{14}$$

If the agricultural production was dependent on the purchase investment in the current watershed to a greater degree, a significant yield reduction would occur.

The total value of the water and soil conservation, material investment, and service investment was calculated using the energy price per unit of land area in the river basin as a reference (Fu et al., 2017). The agricultural production investment value in HTRW was calculated indirectly by the equivalent conversion between the investment and the acquired value. The cost investment for agricultural production in HTRW was ¥ 217.13 E+08 (USD$ 34.12 E+08) (Table 4).

Table 4. Energy prices of agricultural production in HTRW (based on status quo scenario).

Classification	Details	Energy value (Sej/ha)	Price of energy (¥/ha)	Total values (¥ E+08)	Cost investment (¥ E+08)
Water and soil conservation	Soil erosion	3.08E+14	594.53	6.40	6.40
Material investment	Depreciation	3.05E+15	1,960.34	21.10	21.10
	Fuel oil	2.90E+13	18.64	0.20	0.20
	Material	1.42E+16	9,126.83	98.23	98.23
	Labour	1.29E+16	8,291.28	89.24	89.24
Service investment	Maintenance and management	2.51E+14	161.33	1.74	1.74
	Service	3.30E+13	21.21	0.23	0.23
Total				217.13	217.13

To calculate the elasticity of the farmland yield data derived from Eq. (13), the expression was used as follows:

$$(\frac{\mathrm{d}q}{q}) / (\frac{\mathrm{d}A}{A}) = (\frac{217.13E+08}{3800E+08}) / (\frac{29500}{1076300}) = 2 . \quad (15)$$

Here, dq was the farmland production cost after deducting the paid amount, q was the agricultural production value of the farmland, dA was the total reduced area of the farmland under EPS, and A was the total area of the farmland. We obtained the agricultural production value from Liaoning Province statistical yearbooks-2013.

Based on this calculation, to maximize profit, 1% of the currently cultivated or used land in HTRW was converted into preserved land to supply more ecosystem services. Accordingly, the crop yield in HTRW was reduced by 2%. The analysis results based on the ecological land-use value in HTRW, the forestland, grassland, and wetlands were the main suppliers of ecosystem

services. Therefore, the decreased farmland and increased the ecological value of the non-cultivated land were profit indicators.

4. Conclusions

NPS pollution often occurs on dry farmlands and in paddy, rural and urban areas. Many studies have applied the SWAT model to study NPS in China, mainly focusing on scenario simulations of NPS pollution and management in agricultural areas with rich hydrological and meteorological data. Basic monitoring data on HTRW were deficient. Thus, we selected SWAT as a feasible method for assessing NPS pollutant loading at the watershed level. We applied specific practices based on EPS to reduce NPS pollutant loading in the Hunhe, Taizi and Daliao River watersheds. The status quo scenario and EPS were used to calculate the NPS pollutant generation output. NPS pollutant generation output and TN and TP loading were reduced by 22%, 26% and 10% compared with that of the SQS, respectively. The crop yield was reduced by 2% when the land area for ecosystem services in the basin increased by 1%.

The SWAT model can calculate the potential reduction of agricultural NPS pollutants based on different land uses. The reliability of SWAT evaluation results are decided by information completeness and the reasonable degree of parameter initialization. To determine pollutant reduction under different land development patterns and examine the uncertainty of sensitivity parameters, the SWAT model in China has many potential applications. Considering the significance of ecosystem services, much attention should be paid to the relationship between ecosystem service increases and crop yield decreases. Only in this way can ecosystem services and land use be harmoniously developed.

Acknowledgements

The study was financially supported by National Key R&D Program of China (2016YFC0401408), Comprehensive Regulation Theory and Application of Basin Water Environment Process (WE0145B532017), and Project Based Personnel Exchange Program with China Scholarship Council & German Academic Exchange Service of 2015.

References

Abbaspour, K.C., Yang, J., Maximov, I., Siber, R., Bogner, K.: Modelling hydrology and water quality in the pre-alpine/alpine Thur watershed using SWAT, J. Hydrol., 333, 413-430, 2007.

Ahearn, D.S., Sheibley, R.W., Dahlgren, R.A.: Land use and land cover influence on water quality in the last free flowing river draining the western Sierra Nevada, California, J. Hydrol., 313, 234-247, 2005.

Arnold, J., Allen, P.: Automated Methods for Estimating Baseflow and Ground Water Recharge from Streamflow Records. Journal of the American Water Resources Association, 35, 411-424, 1999.

Arnold, J.G., Srinivasan, R., Muttiah, R.S.: Large area hydrologic modelling and assessment. Part I: Model development, Journal of the American Water Resources Association, 34, 73-89, 1998.

Cai,Y., Zhao, D.H., Xu, D.L., Jiang, H., Yu, M.Q.: Influences of Land Use on Sediment Pollution across Multiple Spatial Scales in Taihu Basin, Clean-Soil, Air, Water, 43, 1616-1622, 2015.

Department of Environmental Protection of Liaoning Province: Liaoning Province Environmental Bulletin, 2011.

Ficklin, D.L., Luo, Y.Z., Luedeling, E., Zhang, M.H.: Climate change sensitivity assessment of a highly agricultural watershed using SWAT, J. Hydrol., 374, 16-29, 2009.

Fu, Y.C., Du, X., Ruan, B.Q, Liu, L.S., Zhang, J. Agro-ecological compensation of watershed based on emergy. Water Science & Technology, 76, 2830-2841. 2017.

Gassman, P.W., Reyes, M.R., Green, C.H., Arnold, J.G.: The Soil and Water Assessment Tool: Historical development, applications and future directions, Trans ASABE, 50, 1211-1250, 2007.

Gosain, A.K., Rao, S., Srinivasan, R.: Return-flow assessment for irrigation command in the Palleru River Basin using SWAT model, Hydrol Process,19, 673-682, 2005.

Hao, L.P.: Characteristics of nitrogen and phosphorus losses of rainfall runoff in Liaoning Hunhe Basin, Shenyang Agricultural University, 2012.

Hong, Q., Sun, Z., Chen, L., Liu, R., Shen, Z.: Small-scale watershed extended method for nonpoint source pollution estimation in part of the Three Gorges Reservoir Region, Int J Environ Sci Technol., 9, 595-604, 2012.

649 Lam, Q.D., Schmalz, B., Fohrer, N.: The impact of agricultural Best Management Practices on water quality
650 in a North German lowland catchment, Environ Monit Assess, 183, 351-379, 2011.
651 Lee, M.S., Park, G.A., Park, M.J.: Evaluation of non-point source pollution reduction by applying Best
652 Management Practices using a SWAT model and Quick Bird high resolution satellite imagery, Journal
653 of Environmental Sciences, 22, 826-833, 2010.
654 Li, M., Zhu, B., Hou, Y.L.: Phosphorus release risk on a calcareous purple soil in southwest China, Int J
655 Environ Pollut., 40, 351-362, 2007.
656 Liu, M., Li, C.L., Hu, Y.M., Sun, F.Y.: Combining CLUE-S and SWAT Models to Forecast Land Use Change
657 and Non-Point Source Pollution Impact at a Watershed Scale in Liaoning Province, China. Chin. Geogra.
658 Sci., 24, 540-550, 2014.
659 Logsdon, R.A., Chaubey, I.: A quantitative approach to evaluating ecosystem services, Ecological Modelling,
660 257, 57-65, 2013.
661 Nash, J.E., Sutcliffe, J.V.: River flow forecasting through conceptual models part I-A discussion of principles,
662 J Hydrol.,10, 282-290,1970.
663 Niraula, R., Kalin, L., Srivastava, P., Anderson, C.J.: Identifying critical source areas of nonpoint source
664 pollution with SWAT and GWLF, Ecological Modelling, 268, 123-133, 2013.
665 Outram, F.N., Cooper, R.J., S¨unnenberg, G., Hiscock, K.M., Lovett, A.A.: Antecedent conditions,
666 hydrological connectivity and anthropogenic inputs: factors affecting nitrate and phosphorus transfers
667 to agricultural headwater streams, Sci Total Environ., 545, 184-199, 2016.
668 Ouyang, W., Huang, H., Hao, F.: Synergistic impacts of land-use change and soil property variation on non-
669 point source nitrogen pollution in a freeze-thaw area, J. Hydrol., 495, 126-134, 2013.
670 Ouyang, W., Wang, X., Hao, F.: Temporal-spatial dynamics of vegetation variation on non-point source
671 nutrient pollution, Ecological Modelling, 220, 2702-2713, 2009.
672 Robinson,T.H., Leydecker, A., Keller, A.A.: Steps towards modeling nutrient export in coastal Californian
673 streams with a Mediterranean climate, Agricultural Water Management, 77, 144-158, 2005.
674 Sadeghi, S.H.R., Jalili, K., Nikkami, D.: Land use optimization in watershed scale, Land Use Policy, 26, 186-
675 193, 2009.
676 Shen, Z.Y., Chen, L., Hong, Q.b., Qiu, J.L.: Assessment of nitrogen and phosphorus loads and causal factors
677 from different land use and soil types in the Three Gorges Reservoir Area, Sci Total Environ., 454, 383-
678 392, 2013.
679 Shen, Z.Y., Hong, Q., Yu, H., Niu, J.F.: Parameter uncertainty analysis of non-point source pollution from
680 different land use type, Sci Total Environ., 408, 1971-1978, 2010.
681 Shen, Z.Y., Liao, Q., Hong, Q., Gong, Y.W.: An overview of research on agricultural non-point sources
682 pollution modelling in China, Sep Purif Technol., 9, 595-604, 2011.
683 Simpson, R.D. Ecosystem services as substitute inputs: basic results and important implications for

conservation policy. Ecol Econ. 98, 102-108. 2014.
Vincent, J. R., Binkley, C.S., 1993. Efficient multiple-use forestry may require land-use specialization. Land Econ. 69, 370-376.
Wang, G., Yang, H., Wang, L., Xu, Z., Xue, B.: Using the SWAT model to assess impacts of land use changes on runoff generation in headwaters, Hydrol Process, 28, 1032-1042, 2014.
Wang, X.L., Wang, Q., Wu, C.Q., Liang, T., Zheng, D.H., Wei, X.F.: A method coupled with remote sensing data to evaluate non-point source pollution in the Xin'anjiang catchment of China, Sci Total Environ., 430, 132-143, 2012.
Williams, J.R.: Sediment routing for agricultural watersheds, Water Resour. Bull., 11, 965-974, 1975.
Yang, J., Reichert, P., Abbaspour, K.C., Xia, J., Yang, H.: Comparing uncertainty analysis techniques for a SWAT application to the Chaohe Basin in China, J Hydrol., 358, 1-23, 2008.
Yang, J.L., Zhang, G.L., Zhao, Y.G.: Land use impact on nitrogen discharge by stream: a case study in subtropical hilly region of China, Nutrient Cycling in Agroecosystems, 77, 29-38, 2007.
Yang, Y., Wang, G., Wang, L., Yu, J., Xu, Z.: Evaluation of Gridded Precipitation Data for Driving SWAT Model in Area Upstream of Three Gorges Reservoir, PLOS ONE, 9, e112725. doi: 10.1371/journal.pone.0112725, 2014.
Yin, G., Wang, N., Yuan, X.: Non-point source pollution of nitrogen and phosphorus nutrients using SWAT model in tumen river watershed, China, Journal of Agro-Environment Science, 30, 704-710, 2011.
Zhang, Y.H.: Development of Study on Model-SWAT and Its Application, Progress in Geography, 24, 121-130, 2005.